Constraining the history of reheating with the NANOGrav 15-year data

L. Sriramkumar

Centre for Strings, Gravitation and Cosmology, Department of Physics,
Indian Institute of Technology Madras, Chennai

21st Century Cosmology: Tensions, Anomalies and New Physics

Ashoka University, Sonipat

August 21–23, 2024

Plan of the talk

1. Constraints on inflation from the CMB data
2. Reheating and its effects on primary GWs
3. Generation of GWs by enhanced scalar perturbations on small scales
4. NANOGrav 15-year data and the stochastic GW background
5. Outlook

This talk is based on. . .

- H. V. Ragavendra, P. Saha, L. Sriramkumar and J. Silk, *Primordial black holes and secondary gravitational waves from ultra slow roll and punctuated inflation*, Phys. Rev. D **103**, 083510 (2021) [arXiv:2008.12202 [astro-ph.CO]].
- Md. R. Haque, D. Maity, T. Paul and L. Sriramkumar, *Decoding the phases of early and late time reheating through imprints on primordial gravitational waves*, Phys. Rev. D **104**, 063513 (2021) [arXiv:2105.09242 [astro-ph.CO]].
- S. Maity, N. Bhaumik, Md. R. Haque, D. Maity and L. Sriramkumar, Constraining the history of reheating with the NANOGrav 15-year data, arXiv:2403.16963 [astro-ph.CO].

Plan of the talk

Bringing the modes inside the Hubble radius

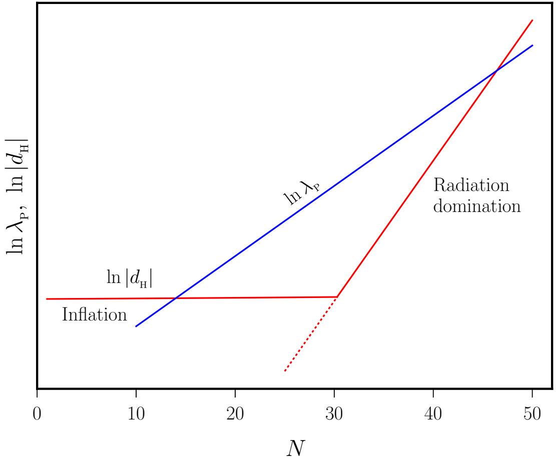

Evolution of comoving lengths

The physical wavelength $\lambda_{\rm P} \propto a$ (in blue) and the Hubble radius $d_{\rm H} = H^{-1}$ (in red) in the inflationary scenario[1]. The scale factor is expressed in terms of e-folds N as $a(N) \propto {\rm e}^N$.

[1] See, for example, E. W. Kolb and M. S. Turner, *The Early Universe* (Addison-Wesley Publishing Company, New York, 1990), Fig. 8.4.

The inflationary attractor

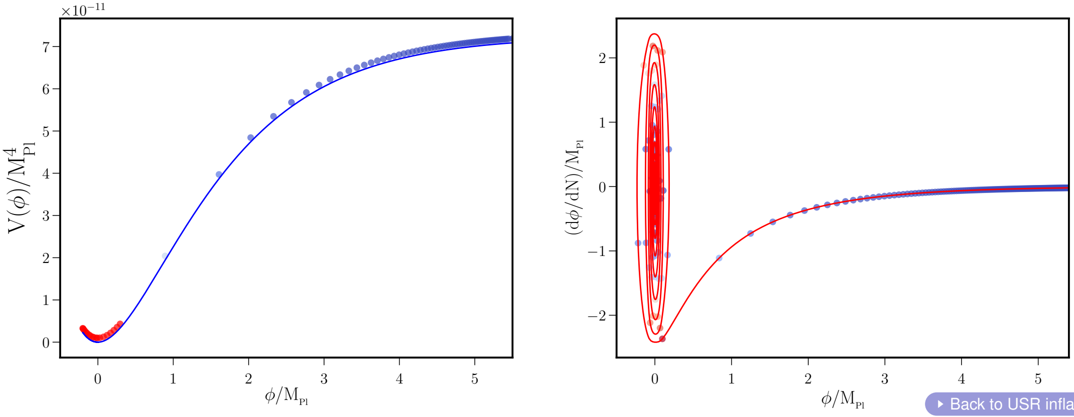

Back to USR inflation
Back to reheating

The evolution of the scalar field in the popular Starobinsky model, which leads to slow roll inflation, is indicated (as circles, in blue and red) at regular intervals of time (on the left). Illustration of the behavior of the scalar field in phase space (on the right)[2].

[2]Figure credit H. V. Ragavendra.

Performance of inflationary models in the n_{s}-r plane

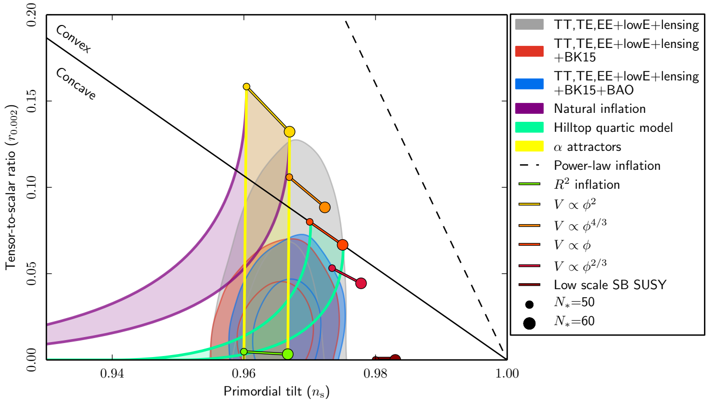

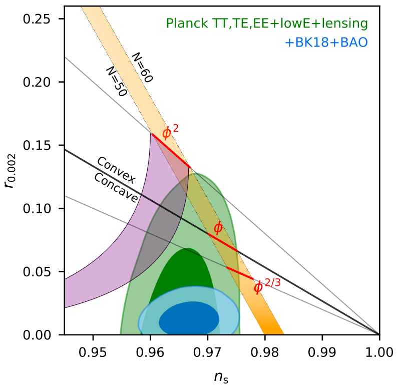

Left: Joint constraints on n_{s} and $r_{0.002}$ from Planck in combination with other data sets, compared to the theoretical predictions of some of the popular inflationary models[3].
Right: Latest constraints on the tensor-to-scalar ratio r from the BICEP/Keck telescopes[4].

[3] Planck Collaboration (Y. Akrami *et al.*), Astron. Astrophys. **641**, A10 (2020).

[4] BICEP/Keck Collaboration (P. A. R. Ade *et al.*), arXiv:2203.16556 [astro-ph.CO].

Plan of the talk

Behavior of the comoving wave number and Hubble radius

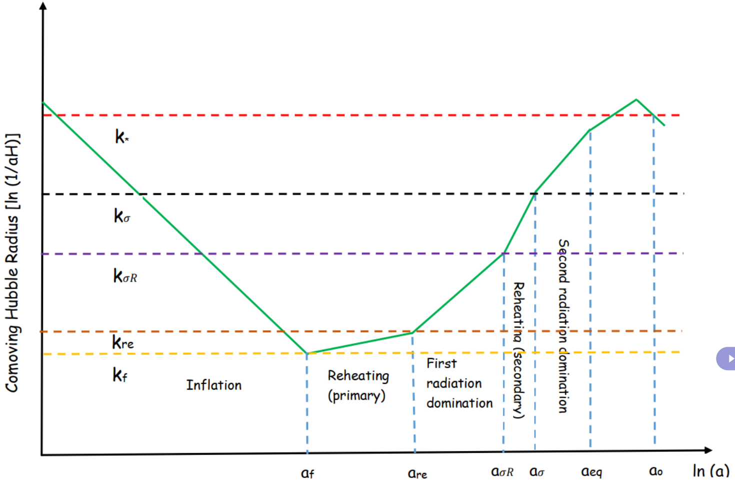

Evolution of physical lengths
Inflationary attractor
Back to secondary GWs

Behavior of the comoving wave number k (horizontal lines in different colors) and the comoving Hubble radius $d_{\mathrm{H}}/a = (a\,H)^{-1}$ (in green) across different epochs[5].

[5] Md. R. Haque, D. Maity, T. Paul and L. Sriramkumar, Phys. Rev. D **104**, 063513 (2021).

Duration of reheating and the reheating temperature

The duration of the epoch of reheating N_{re} and the reheating temperature T_{re} can be expressed in terms of the equation of state parameter w_{re} during reheating and the inflationary parameters as follows[6]:

$$N_{\mathrm{re}} = \frac{4}{(3\,w_{\mathrm{re}}-1)}\left[N_{*}+\frac{1}{4}\,\ln\left(\frac{30}{\pi^2\,g_{*,\mathrm{re}}}\right)+\frac{1}{3}\,\ln\left(\frac{11\,g_{s,\mathrm{re}}}{43}\right)+\ln\left(\frac{k_*}{a_0\,T_0}\right)+\ln\left(\frac{\rho_{\mathrm{e}}^{1/4}}{H_{\mathrm{I}}}\right)\right],$$

$$T_{\mathrm{re}} = \left(\frac{43}{11\,g_{s,\mathrm{re}}}\right)^{1/3}\left(\frac{a_0\,H_{\mathrm{I}}}{k_*}\right)\,\mathrm{e}^{-(N_*+N_{\mathrm{re}})}\,T_0,$$

where H_{I} is the Hubble parameter during inflation, $T_0 = 2.725\,\mathrm{K}$ is the present temperature of the CMB, and H_0 denotes the current value of the Hubble parameter.

Note that $k_*/a_0 \simeq 0.05\,\mathrm{Mpc}^{-1}$ represents the CMB pivot scale and N_* denotes the number of e-folds *prior to the end of inflation* when the pivot scale leaves the Hubble radius.

[6] J. Martin and C. Ringeval, Phys. Rev. D **82**, 023511 (2010);
L. Dai, M. Kamionkowski and J. Wang, Phys. Rev. Lett. **113**, 041302 (2014);
J. L. Cook, E. Dimastrogiovanni, D. A. Easson and L. M. Krauss, JCAP **04**, 047 (2015).

Probing the primordial universe through GWs

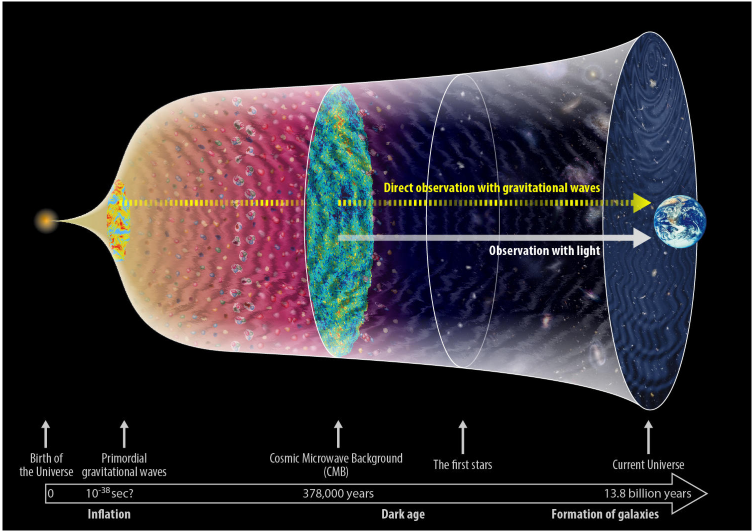

GWs provide a unique window to probe the primordial universe[7].

[7] Image from https://gwpo.nao.ac.jp/en/gallery/000061.html.

The spectrum of GWs

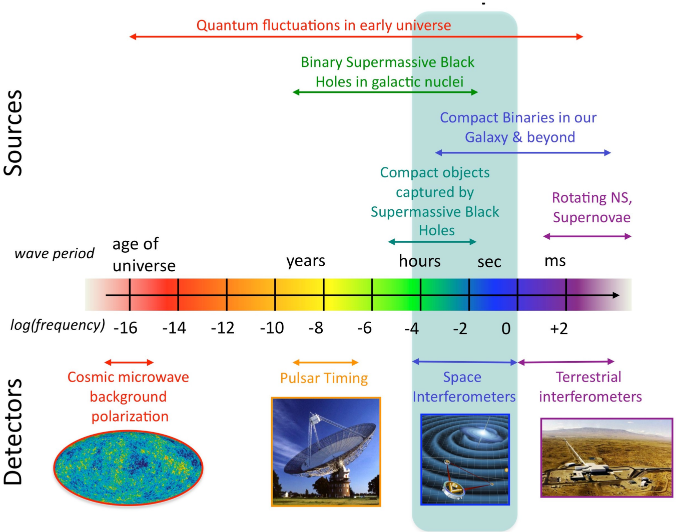

Different sources of GWs and corresponding detectors[8].

[8] J. B. Hartle, *Gravity: An Introduction to Einstein's General Relativity* (Pearson Education, Delhi, 2003).

Effects on $\Omega_{\rm GW}(f)$ due to reheating

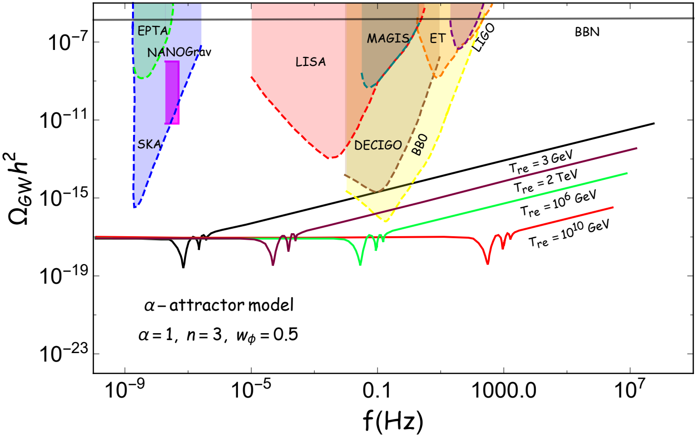

The behavior of the dimensionless spectral energy density of primary GWs today, viz. $\Omega_{\rm GW}$, is plotted, over a wide range of frequency f, for different reheating temperatures (in red, green, brown and black)[9].

[9]See, for example, K. Nakayama, S. Saito, Y. Suwa and J. Yokoyama, JCAP **0806** 020 (2008); Md. R. Haque, D. Maity, T. Paul and L. Sriramkumar, Phys. Rev. D **104**, 063513 (2021).

Effects on $\Omega_{\rm GW}(f)$ due to late time entropy production

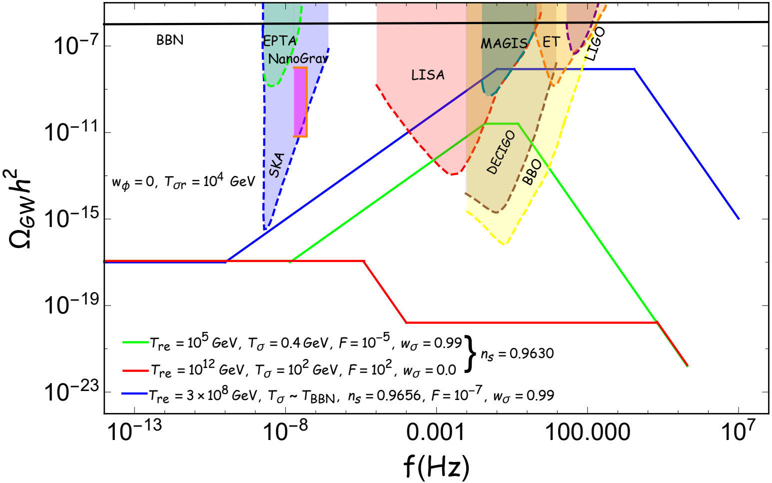

The dimensionless spectral energy density of primary GWs observed today $\Omega_{\rm GW}(f)$ is plotted in scenarios involving late time production of entropy[10].

[10] Md. R. Haque, D. Maity, T. Paul and L. Sriramkumar, Phys. Rev. D **104**, 063513 (2021).

Plan of the talk

Production of primordial black holes (PBHs) during radiation domination

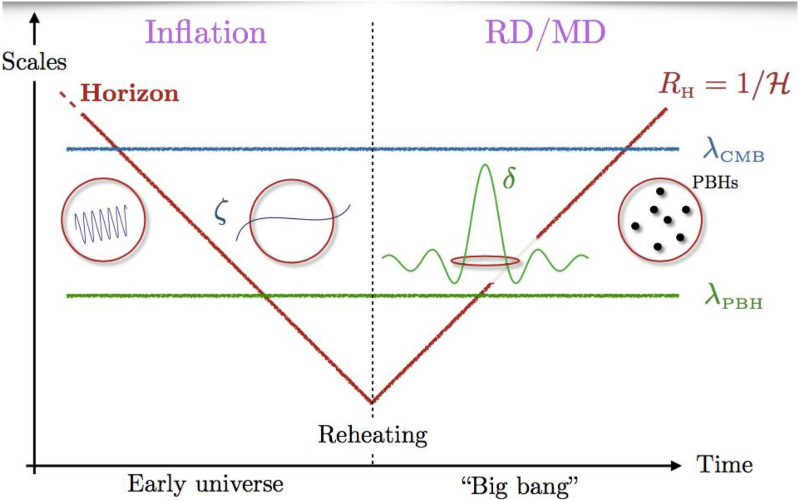

BHs can form in the primordial universe when perturbations with significant amplitudes on small scales reenter the Hubble radius during the radiation dominated epoch[11].

[11] Figure from G. Franciolini, arXiv:2110.06815 [astro-ph.CO].

Amplitude required to form significant number of PBHs

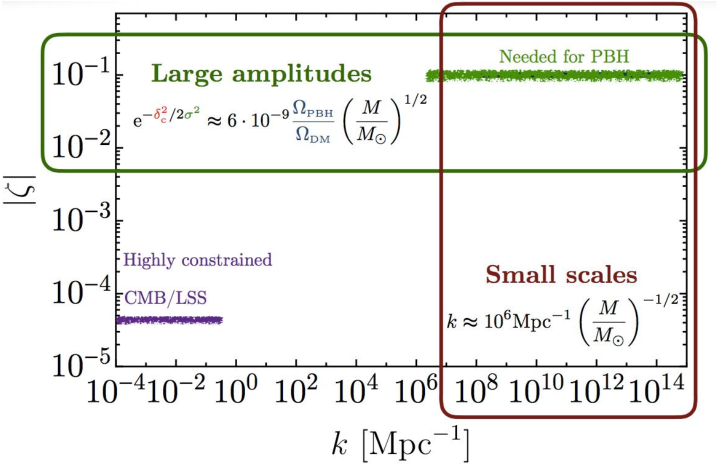

In order to form significant number of black holes, the amplitude of the perturbations on small scales has to be large enough such that the dimensionless amplitude of the scalar perturbation is close to unity[12].

[12] Figure credit G. Franciolini.

Single-field models admitting ultra slow roll inflation

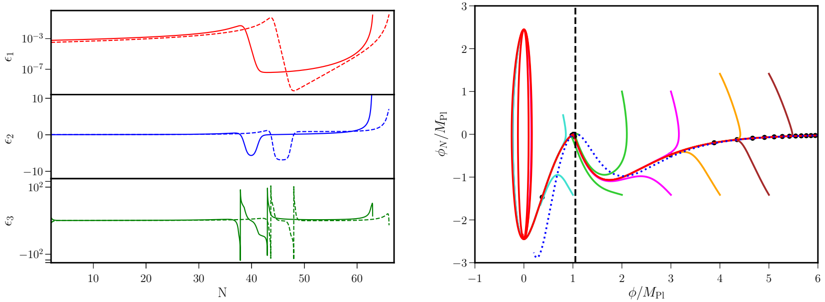

Potentials containing a point of inflection and leading to ultra slow roll inflation[13]: ▸ Inflationary attractor

$$\text{USR1}: V(\phi) = V_0\, \frac{6\,x^2 - 4\,\alpha\, x^3 + 3\, x^4}{(1+\beta\, x^2)^2}, \text{ with } x = \phi/v,\ v \text{ being a constant},$$

$$\text{USR2}: V(\phi) = V_0\, \left\{\tanh\left(\frac{\phi}{\sqrt{6}\, M_{_{\rm Pl}}}\right) + A\, \sin\left[\frac{\tanh\left[\phi/\left(\sqrt{6}\, M_{_{\rm Pl}}\right)\right]}{f_\phi}\right]\right\}^2.$$

[13] See, for example, J. Garcia-Bellido and E. R. Morales, Phys. Dark Univ. **18**, 47 (2017); C. Germani and T. Prokopec, Phys. Dark Univ. **18**, 6 (2017); I. Dalianis, A. Kehagias and G. Tringas, JCAP **01**, 037 (2019).

Power spectra in ultra slow roll and punctuated inflation

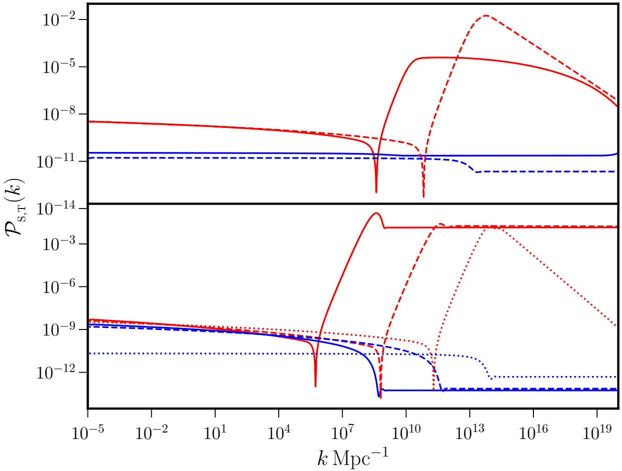

The scalar (in red) and the tensor power (in blue) spectra arising in different ultra slow roll and punctuated inflationary models[14].

Back to analytical form for the power spectrum

[14] H. V. Ragavendra, P. Saha, L. Sriramkumar and J. Silk, Phys. Rev. D **103**, 083510 (2021).

$f_{\rm PBH}(M)$ in ultra slow roll and punctuated inflation

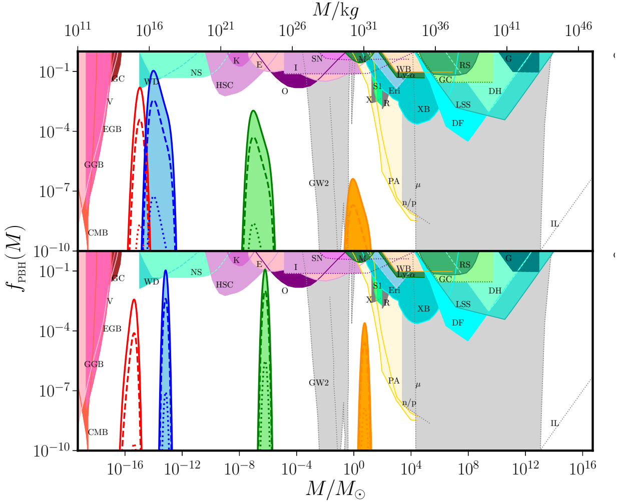

The fraction of PBHs contributing to the cold dark matter density today $f_{\rm PBH}(M)$ has been plotted for different models, viz. USR2 (on top, in red) and PI3 (at the bottom, in red)[15].

[15] H. V. Ragavendra, P. Saha, L. Sriramkumar and J. Silk, Phys. Rev. D **103**, 083510 (2021).

$\Omega_{\rm GW}(f)$ in ultra slow roll and punctuated inflation

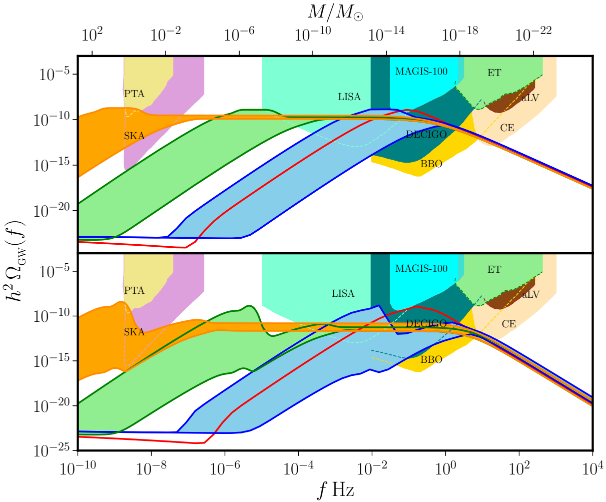

The dimensionless spectral density of GWs $\Omega_{\rm GW}(f)$ arising in the models of USR2 (in red, on top) as well as PI3 (in red, at the bottom)[16].

[16] H. V. Ragavendra, P. Saha, L. Sriramkumar and J. Silk, Phys. Rev. D **103**, 083510 (2021).

Plan of the talk

Hellings-Downs curve

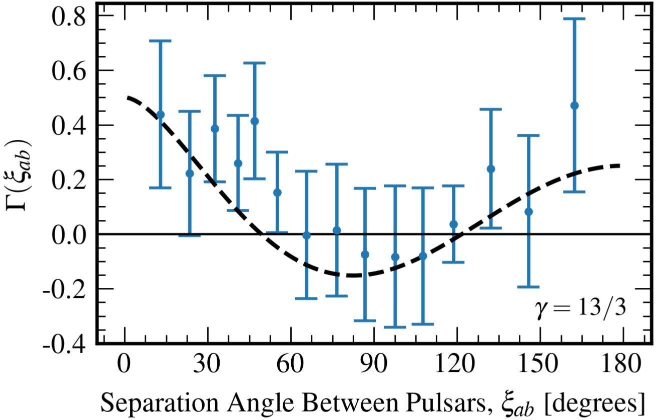

The inter-pulsar correlations measured from 2,211 distinct pairings in the 67-pulsar array of the NANOGrav 15-year data. The dashed black line shows the Hellings-Downs correlation pattern[17].

[17] NANOGrav Collaboration (G. Agazie *et al.*), Astrophys. J. Lett. **951**, 1 (2023); For related discussion, see J. Yokoyama, arXiv:2105.07629 [gr-qc].

Constraints on the spectral amplitude and index of GWs

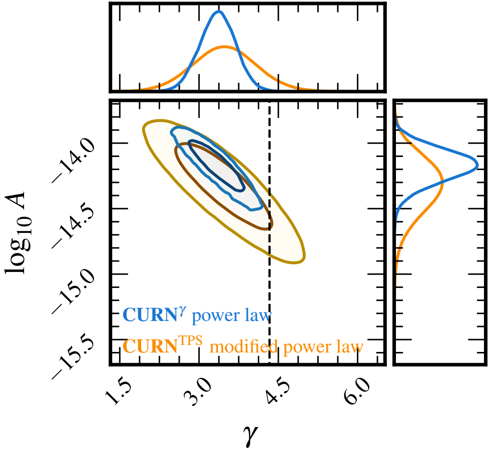

Constraints on the amplitude A and the index γ of the stochastic background of GWs from the NANOGrav 15-year data[18].

[18] NANOGrav Collaboration (G. Agazie *et al.*), Astrophys. J. Lett. **951**, 1 (2023).

Stochastic GW background observed by pulsar timing arrays (PTAs)

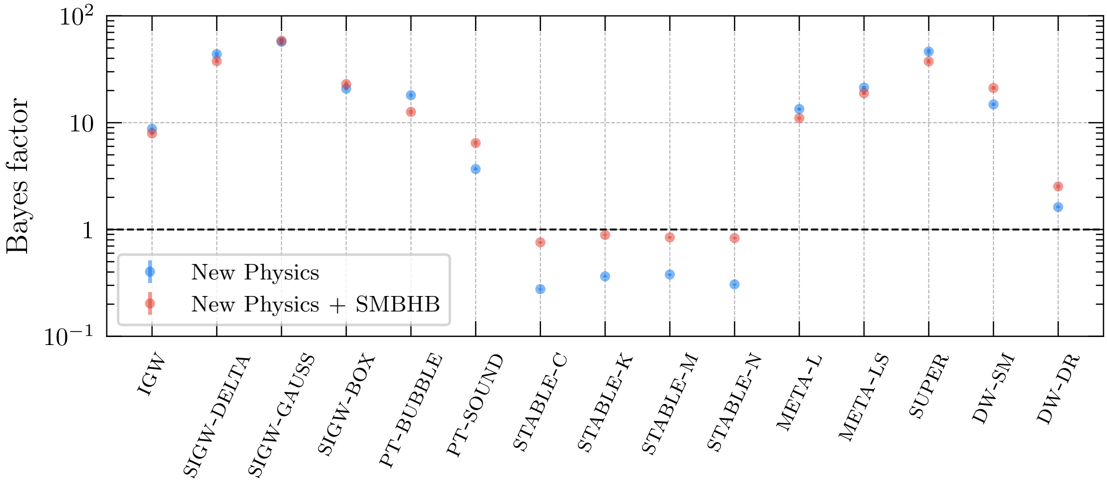

The Bayesian evidence for a variety of astrophysical and cosmological sources for the stochastic GW background suggested by the observations of the PTAs[19].

[19] NANOGrav Collaboration (G. Agazie *et al.*), Astrophys. J. Lett. **951**, 1 (2023).

Shape of the inflationary scalar power spectrum

We assume that the inflationary scalar power spectrum is given by[20]

$$\mathcal{P}_{\rm S}(k) = A_{\rm S}\left(\frac{k}{k_*}\right)^{n_{\rm S}-1} + A_0 \begin{cases} \left(\frac{k}{k_{\rm peak}}\right)^4 & k \leq k_{\rm peak} \\ \left(\frac{k}{k_{\rm peak}}\right)^{n_0} & k \geq k_{\rm peak} \end{cases},$$

where $A_{\rm S}$ and $n_{\rm S}$ are the amplitude and spectral index of the power spectrum at the CMB pivot scale of $k_* = 0.05\,{\rm Mpc}^{-1}$.

▸ Power spectra in USR inflation

We set the reheating temperature to the rather low value of $T_{\rm re} = 50\,{\rm MeV}$.

We shall assume that the threshold value of the density contrast for the formation of PBHs is given by[21]:

$$\delta_{\rm c}^{\rm an} = \frac{3\,(1+w_{\rm re})}{5+3\,w_{\rm re}}\,\sin^2\left(\frac{\pi\,\sqrt{w_{\rm re}}}{1+3\,w_{\rm re}}\right).$$

[20] For other forms of spectra, see G. Domènech, S. Pi, A. Wang and J. Wang, arXiv:2402.18965 [astro-ph.CO].

[21] In this context, see T. Harada, C.-M. Yoo, and K. Kohri, Phys. Rev. D **88**, 084051 (2013).

Formation of PBHs during the phase of reheating

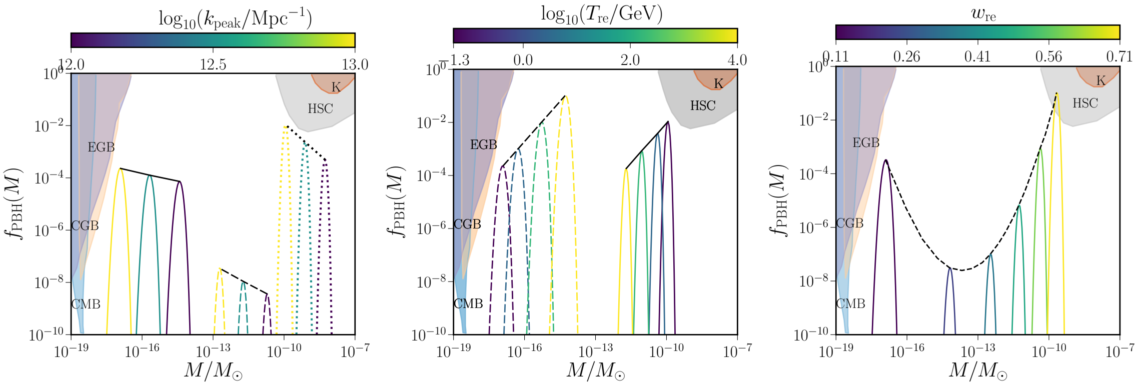

The quantity $f_{\rm PBH}$ is plotted as a function $M/M_\odot$ for a range of $k_{\rm peak}$, $T_{\rm re}$ and $w_{\rm re}$ (in the left, middle and right panels).

Generation of secondary GWs during the epoch of reheating

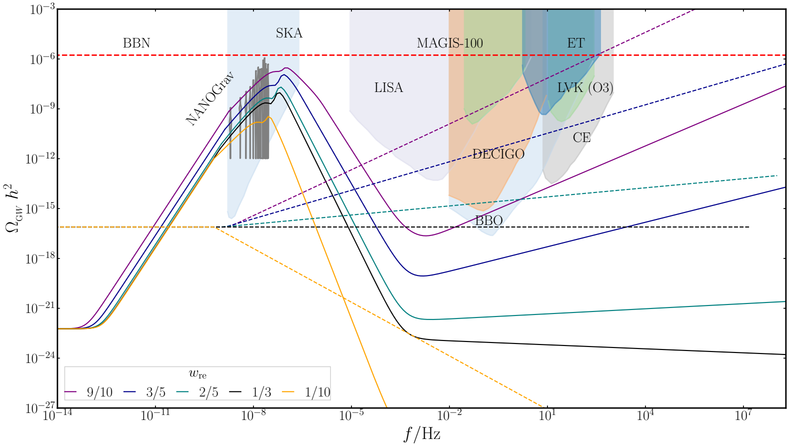

Epoch of reheating

The dimensionless spectral energy density of primary and secondary GWs today $\Omega_{\rm GW}(f)$ is plotted for a given reheating temperature and different values of the parameter describing the equation of state during reheating[22].

[22] S. Maity, N. Bhaumik, Md. R. Haque, D. Maity and L. Sriramkumar, arXiv:2403.16963 [astro-ph.CO].

Best-fit values

Model	Parameter	Prior	Mean value		
R4pF	$\log_{10}\left(\frac{k_{\rm peak}}{\rm Mpc^{-1}}\right)$	$[6, 9]$	$7.62^{+0.35}_{-0.41}$		
	$\log_{10}(A_0)$	$[-3, 0]$	$-1.23^{+0.38}_{-0.66}$		
	$w_{\rm re}$	$[0.1, 0.9]$	0.52 ± 0.23		
	n_0	$[-3.0, -1.5]$	-2.26 ± 0.43		
R3pF	$\log_{10}\left(\frac{k_{\rm peak}}{\rm Mpc^{-1}}\right)$	$[6, 9]$	$7.54^{+0.36}_{-0.44}$		
	$\log_{10}(A_0)$	$[-3, 0]$	$-1.26^{+0.26}_{-0.64}$		
	$w_{\rm re}$	$[0.1, 0.9]$	$0.55^{+0.39}_{-0.14}$		
			$\mathbf{0.5\,\delta_c^{an}}$	$\boldsymbol{\delta_c^{an}}$	$\mathbf{1.5\,\delta_c^{an}}$
R3pB	$\log_{10}\left(\frac{M}{M_\odot}\right)$	$[-6, 3.5]$	$-0.12^{+0.28}_{-0.15}$	$-1.18^{+0.35}_{-0.39}$	$-1.85^{+0.49}_{-0.30}$
	$\log_{10}(f_{\rm PBH})$	$[-20, 0]$	$-0.67^{+0.68}_{-0.16}$	$-6.6^{+6.5}_{-1.9}$	$-10.2^{+8.2}_{-9.6}$
	$w_{\rm re}$	$[0.1, 0.9]$	$0.78^{+0.11}_{-0.030}$	$0.66^{+0.23}_{-0.19}$	0.55 ± 0.17
R2pB	$\log_{10}\left(\frac{M}{M_\odot}\right)$	$[-6, 3.5]$	$-0.24^{+0.38}_{-0.45}$	$-1.60^{+0.16}_{-0.14}$	$-2.45^{+0.20}_{-0.13}$
	$w_{\rm re}$	$[0.1, 0.9]$	$0.77^{+0.13}_{-0.038}$	0.59 ± 0.16	$0.464^{+0.095}_{-0.25}$

The best-fit values arrived at upon comparison with the NANOGrav 15-year data.

Constraints on the epoch of reheating

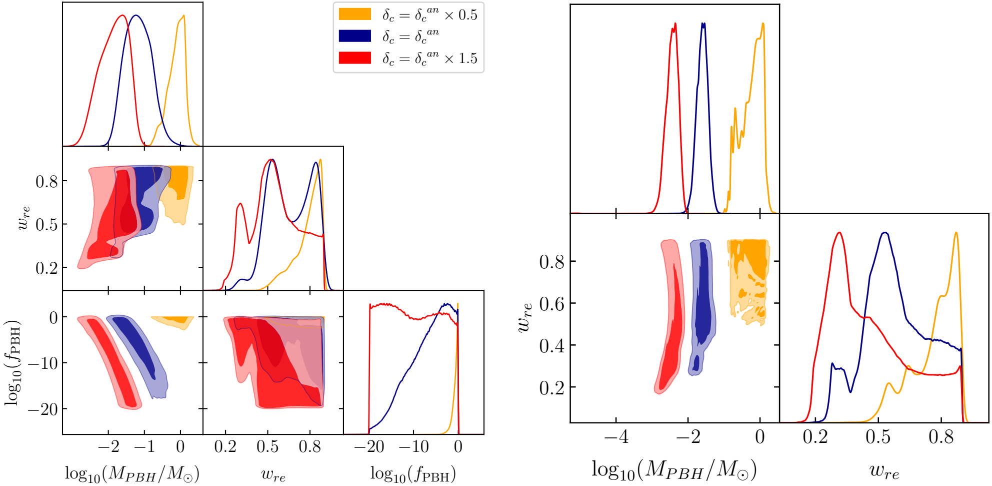

Constraints on the parameters in the models `R3pB` (on the left) and `R2pB` (on the right), arrived at upon comparison with the NANOGrav 15-year data[23].

[23] S. Maity, N. Bhaumik, Md. R. Haque, D. Maity and L. Sriramkumar, arXiv:2403.16963 [astro-ph.CO].

Generation of secondary GWs during the epoch of reheating

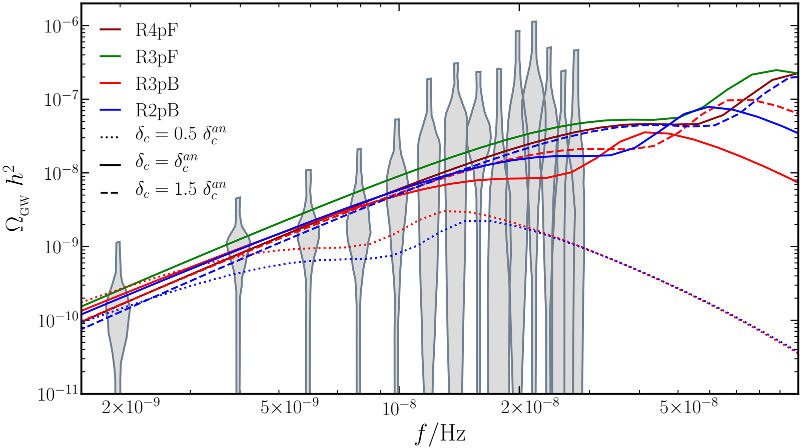

The dimensionless spectral energy density of the secondary GWs today $\Omega_{\rm GW}(f)$ is plotted for a given reheating temperature and the best-fit values of the parameters in the different models[24].

[24] S. Maity, N. Bhaumik, Md. R. Haque, D. Maity and L. Sriramkumar, arXiv:2403.16963 [astro-ph.CO].

Extent of PBHs formed

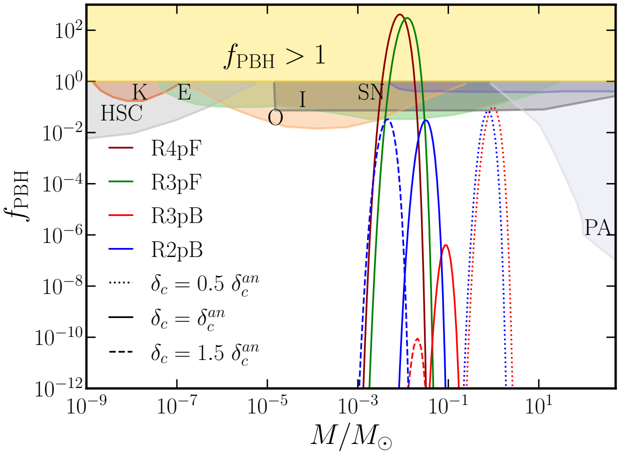

The fraction of PBHs that constitute the dark matter density today, viz. $f_{\rm PBH}(M)$ is plotted for a given reheating temperature and the best-fit values of the parameters in the different models[25].

[25] S. Maity, N. Bhaumik, Md. R. Haque, D. Maity and L. Sriramkumar, arXiv:2403.16963 [astro-ph.CO].

Bayesian evidence

Model X	Model Y	$\mathrm{BF}_{Y,X}$		
		$\delta_c = 0.5\,\delta_c^{\mathrm{an}}$	$\delta_c = \delta_c^{\mathrm{an}}$	$\delta_c = 1.5\,\delta_c^{\mathrm{an}}$
SMBHB	R2pB	$1.7 \pm .06$	260.04 ± 19.21	350.61 ± 27.36

The Bayesian factors $\mathrm{BF}_{Y,X}$ for the model R2pB that invokes primordial physics as the source of the stochastic GW background observed by the NANOGrav 15-year data, when compared to the astrophysical SMBHB model.

Bayesian factors $\mathrm{BF}_{Y,X}$ that far exceed unity indicate strong evidence for the model Y with respect to the model X.

Clearly, when $\delta_c = \delta_c^{\mathrm{an}}$ and $\delta_c = 1.5\,\delta_c^{\mathrm{an}}$, the NANOGrav 15-year data strongly favors the model R2pB when compared to the SMBHM model.

Plan of the talk

Outlook

- If one of the future CMB missions—such as LiteBIRD (Lite, Light satellite for the studies of B-mode polarization and Inflation from cosmic background Radiation Detection), Primordial Inflation Explorer (PIXIE) or Exploring Cosmic History and Origin (ECHO, a proposed Indian effort)—detect the signatures of the primordial GWs, it will help us arrive at strong constraints on the dynamics during inflation and reheating.
- The observations by LIGO have opened up a new window to observe the universe.
- The observations by the PTAs and their possible implications for the stochastic GW background offer a wonderful opportunity to understand the physics operating over a wider range of scales in the early universe. During the coming decades, GW observatories such as the Laser Interferometer Space Antenna (LISA), Einstein Telescope and Cosmic Explorer, can be expected to provide us with an unhindered view of the primordial universe.

Collaborators

H. V. Ragavendra

Pankaj Saha

Joseph Silk

Md. Riajul Haque

Debaprasad Maity

Tanmoy Paul

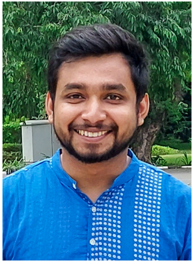

Suvashis Maity

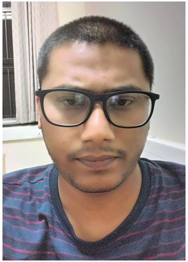

Nilanjandev Bhaumik

Thank you for your attention